Journal of Alloys and Compounds 583 (2014) 488–491

Contents lists available at ScienceDirect

Journal of Alloys and Compounds

journal homepage: www.elsevier.com/locate/jalcom

Red shift and higher photoluminescence emission of CCTO thin films undergoing pressure treatment

T. Sequinel [a,*], I.G. Garcia [a], S.M. Tebcherani [b], E.T. Kubaski [c,1], L.H. Oliveira [a], M. Siu Li [d], E. Longo [a], J.A. Varela [a]

[a] Instituto de Química, UNESP, Rua Prof. Francisco Degni 55, 14800-900 Araraquara, SP, Brazil
[b] Departamento de Engenharia de Produção, UTFPR, Av. Monteiro Lobato, s/n – Km 04, 84016-210 Ponta Grossa, PR, Brazil
[c] Itajara Minérios Ltda., Rua Balduíno Taques 170, 84010-050 Ponta Grossa, PR, Brazil
[d] Instituto de Física, USP, Av. Trabalhador são-carlense, 400, 13566-590 São Carlos, SP, Brazil

ARTICLE INFO

Article history:
Received 20 June 2013
Received in revised form 29 August 2013
Accepted 30 August 2013
Available online 10 September 2013

Keywords:
CCTO
Thin films
Pressure method
Photoluminescence

ABSTRACT

CCTO thin films were deposited on Pt(1 1 1)/Ti/SiO_2/Si substrates using a chemical (polymeric precursor) and pressure method. Pressure effects on CCTO thin films were evaluated by X-ray diffraction (XRD), field emission scanning electron microscopy (FE-SEM) and optical properties which revealed that a pressure film (PF) is denser and more homogeneous than a chemical film (CF). Pressure also causes a decrease in the band gap and an increase in the photoluminescence (PL) emission of CCTO films which suggests that the pressure facilitates the displacement of Ti in the titanate clusters and the charge transference from TiO_6 to $[TiO_5V_0^z]$, $[TiO_5V_0^z]$ to $[CaO_{11}V_0^z]$ and $[TiO_5V_0^z]$ to $[CuO_4]^x$.

1. Introduction

Calcium copper titanate ($CaCu_3Ti_4O_{12}$ – CCTO) has attracted much attention and is becoming an important material for device applications due to its high dielectric constant at room temperature ($\sim 10^5$) which is nearly constant from 100 to 600 K [1–3]. The CCTO structure is a variation of the perovskite structure ($AB_3Ti_4O_{12}$) which possesses TiO_6 octahedra clusters and has a square planar coordination with B [4]. The perovskite structure can be considered flexible, and most of the distortion on this structure is based on tilting of TiO_6 octahedra which causes a displacement in the 180° angles of O–Ti–O bonds [4]. The disordered structure of the perovskite contributes to PL emission at room temperature; this effect can be observed by exciting the material with wavelengths of higher energy than the band gap [5].

The PL of disordered perovskite has been studied since the first visible PL at room temperature was observed in porous silicon [6]. The order–disorder structure is one of the most accepted models to explain titanate crystalline PL emission at room temperature [7–9]. In general, neither completely ordered nor completely disordered systems exhibit PL; consequently, a medium range order–disorder is necessary for PL emission [10–12]. Materials with enhanced PL properties are interesting for their high resolution and efficient waveguides in lamps and optical devices such as integrated light emission devices and field emission displays [13].

CCTO is a body-centered cubic (bcc) perovskite; optical properties of this material are due to two main factors: (1) the order–disorder of TiO_6 and $TiO_5V_0^z$ clusters where V_0^z is the oxygen vacancies (V_0^x, $V_0^{\cdot}$ and $V_0^{\cdot\cdot}$). TiO_6 clusters should be linked with CaO_{12} and CuO_4. However, literature reports note that the strong green (500–570 nm) emission of CCTO is associated with a charge transfer from TiO_6 to $(TiO_5V_0^z)$, $(TiO_5V_0^z)$ to $(CaO_{11}V_0^z)$ and $(TiO_5V_0^z)$ to $(CuO_4)^x$ [5,14]. (2) Other authors also reported that the CCTO emission could originate from the Ti off-center displacement along ⟨111⟩ directions which is common to TiO_6 clusters [1].

To decrease the cost of several electronic and optical devices, it is important to obtain higher PL emission and a low synthesis temperature. Based on these facts, to improve the CCTO PL emission and reduce the temperature of thin film deposition, the aim of this study is to obtain CCTO thin films formed by using two different methods: chemical [15] and pressure [16–19] depositions.

2. Material and methods

Calcium carbonate (Aldrich, 99.999%), copper carbonate basic (Aldrich, 99.99%), titanium isopropoxide (Aldrich, 99.999%), ethylene glycol (Synth, 99%) and citric acid (Aldrich, 99.5%) were used as starting materials in the synthesis of the CCTO polymeric solution. The CCTO solution viscosity was controlled to about 20 cP using

* Corresponding author. Tel.: +55 16 3301 9828.
E-mail address: sequinel.t@gmail.com (T. Sequinel).
[1] Present address: State University of Ponta Grossa, Av. General Carlos Cavalcanti 4748, 84030-900 Ponta Grossa, PR, Brazil.

0925-8388/$ - see front matter © 2013 Elsevier B.V. All rights reserved.
http://dx.doi.org/10.1016/j.jallcom.2013.08.210

water and was measured using a Brookfield viscometer. CFs [15] were synthesized by spinning the polymeric solution on the substrate surface at 4000 rpm for 30 s; this procedure was repeated layer by layer five times. CFs were treated at 340 °C for 4 h to remove the organic matter; then CFs were annealed at 500 °C, 600 °C and 700 °C for 32 h in a conventional furnace under an ambient atmosphere.

Another group of CCTO thin films was deposited on Pt(1 1 1)/Ti/SiO_2/Si substrates by the pressure method. The thin film deposition methodology using pressure can be found elsewhere in the literature [16–19]. The CCTO powder obtained by the polymeric precursor solution was deposited on substrates, and PFs were synthesized at 340 °C with 2 MPa of pressure in air for 32 h. To study the pressure effect in the CCTO chemical film, after the thermal annealing at 500 °C, 600 °C and 700 °C for 32 h, the CFs were also annealed under a pressure treatment at 340 °C with 2 MPa of pressure in air for 32 h, resulting in the CF + PT films.

CF, CF + PT and PF were characterized by XRD (Rigaku, Model RINT2000) using Cu Kα radiation with the patterns recorded in the 20–80° 2θ measuring range using a step of 0.02° with a measuring time of 0.6 s. The CCTO thin film morphology was obtained by field emission gun electron microscopy (FE-SEM) (JEOL, Model 7500F). PL measurements of CF, CF + PT and PF were performed with a Thermo Jarrel Ash Monospec (27 cm) monochromator coupled to a R955 Hamamatsu photomultiplier using a krypton ion laser (Coherent Innova 200) operating at a wavelength of 350 nm and 60 mW output power. Ultraviolet–visible (UV–vis) absorption spectra were taken using a Varian Cary 5G spectrophotometer to determine the band gap of CCTO thin films; the band gap was estimated using the Kubelka–Munk method [20]. All these characterizations were performed at room temperature.

3. Results and discussion

Fig. 1 shows XRD patterns for both CCTO powders obtained at 900 °C and thin films deposited at different temperatures on Pt(1 1 1)/Ti/SiO_2/Si substrate surface. Fig. 1(a) shows well defined diffraction peaks of CCTO powder with a cubic structure which belongs to the *Im-3* space group (JCPDS 75-1149). CFs annealed at 500 °C show no CCTO reflection, and only platinum and silicon substrate peaks (marked with an *), can be observed (see Fig. 1(b)) which indicates that an amorphous CCTO film was obtained under these conditions. This result was confirmed by morphological features and optical properties. On the other hand, CFs treated at 500 °C under the influence of pressure revealed the CCTO main reflection peak (2 2 0); i.e., the CCTO film became crystalline after pressure treatment (see Fig. 1(c)) and shows the first effect of pressure on the synthesis film. All other CCTO films (CF at higher temperatures, CF + PT and PF) (see Fig. 1(d–h)) also showed the crystalline reflection peak (2 2 0) (JCPDS 75-1149).

Fig. 2 illustrates the morphological features of CCTO thin film surfaces that were characterized by FEG-SEM. An analysis of the surface morphology reveals that both CFs and PFs show a porous surface (see Fig. 2(a)–(c)); however, PFs have larger grain sizes

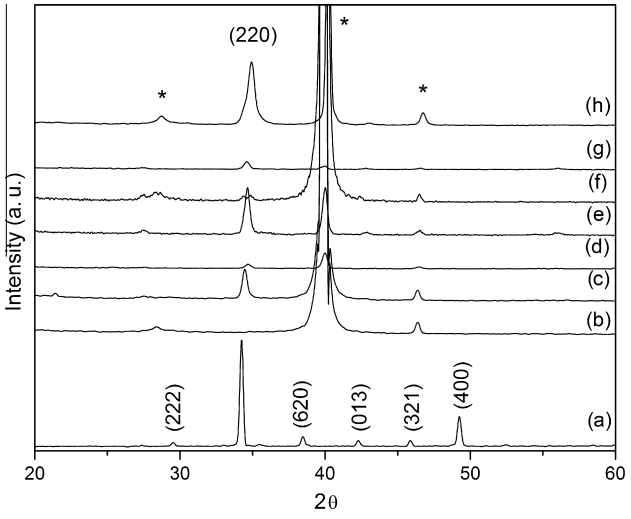

Fig. 1. XRD patterns for CCTO powders obtained at 900 °C and thin films deposited at different temperatures. (a) CCTO powder; (b) CF-500 °C; (c) CF-500 °C + PT; (d) CF-600 °C; (e) CF-600 °C + PT; (f) CF-700 °C; (g) CF-700 °C + PT; (h) PF.

(from the CCTO powder) and denser films (see Fig. 2(d)). In addition, the CF-500 °C film (see Fig. 2(a)) showed no grain growth and corroborates the amorphous phase in XRD patterns (see Fig. 1(b)). Thermal CFs annealed at different temperatures produced CCTO film growth parameters starting with crystallization and grain coalescence at 600 °C (see Fig. 2(b)) and finishing with CCTO CF growth at only 700 °C (see Fig. 2(c)). By studying for CCTO thin film surface morphologies, we conclude that PFs require lower temperatures to reach larger grain sizes as well as denser, and more crystalline films than the results obtained by spinning the chemical solution onto the substrate. CF + PT surface morphologies were similar to CF surface morphologies which indicates that pressure affected only the internal structure.

To evaluate the effect of pressure on CCTO thin film structures, the PL signal for all films synthesized was studied. A comparison of the PL emission of CF with CF + PT synthesized at different temperatures is shown in Fig. 3.

As illustrated in Fig. 3(a), the CCTO CFs have a maximum PL emission at around 450 nm (blue region) but no significant dependence in PL spectra due to different conditions of thermal annealing. Conversely, a red shift in PL spectra was observed after pressure treatment (see Fig. 3(b)) which resulted in a displacement of the PL maximum emission to the green region (500–560 nm). Furthermore, pressure treatment increased the intensity of the PL emission and reached the highest PL emission in CF-500 °C + PT (about two order of magnitude higher than when no pressure treatment was conducted). The amorphous CCTO film obtained at 500 °C resulted in a more resilient film to the pressure effect which favored the medium disorder of clusters $TiO_5V_0^z$.

The effect of pressure on the order–disorder of CCTO film clusters can be represented by Kröger-Vink [21] notation. Eq. (1) represents cluster notations to CCTO CF. Conventional furnace annealing produced ordered TiO_6 and $TiO_5V_0^z$ clusters; a disordered $TiO_5V_0^z$ cluster was obtained only after pressure treatment (Eq. (2)). The disordered octahedral $[TiO_5V_0^x]_d$ represents the high PL emission observed to CF + PT (see Fig. 3(b)).

$$\begin{aligned}[TiO_6]_0^x + [TiO_5V_{0]0}^x &\rightarrow [TiO_6]_0' + [TiO_5V_0]_0\\ [TiO_6]_0^x + [TiO_5V_0^{\cdot}]_0 &\rightarrow [TiO_6]_0' + [TiO_5V_0^{\cdot\cdot}]_0\end{aligned} \quad (1)$$

$$\begin{aligned}[TiO_6]_0^x + [TiO_5V_{0]d}^x &\rightarrow [TiO_6]_0' + [TiO_5V_0]_d\\ [TiO_6]_0^x + [TiO_5V_0^{\cdot}]_d &\rightarrow [TiO_6]_0' + [TiO_5V_0^{\cdot\cdot}]_d\end{aligned} \quad (2)$$

The red shift observed in the PL emission after pressure treatment could be justified by the band gap (E_{gap}). The Kubelka–Munk method [20] employed in this work uses the diffuse reflectance spectroscopy to obtain a better accuracy in values for crystalline and amorphous thin films. Maximum PL emission and direct E_{gap} for all CCTO thin films are listed in Table 1.

Moura et al. [22] proposed that an increase in PL emission is caused by a decrease in the CCTO band gap originated from structural defects. Intermediate levels are created inside the band gap by an overlap between the *2p* orbital of oxygen vacancies to the *4d* orbital of titanium. Moura et al. [22] reported an E_{gap} of about 1.63 eV to a ordered film comparable to the CCTO CF-700 °C of this study. Similar to temperature effect described by Moura et al. [22], the smaller E_{gap} observed to the CF + PT reported here indicates that the increase in oxygen pressure can also break the Ti–O bond leading to the origin of $TiO_5V_0^z$ cluster which resulted in an overlap of *2p* orbitals from the oxygen vacancies to the conduction band. The band gap reduction (about 1.1 eV) obtained after the air pressure treatment favors the red shift in the PL emission which involves lower PL emission energy.

Due to a broad band emission in PL spectra (see Fig. 3), the broad band decomposition using the Peakfit Program (version 4.05) was performed. The Gaussian function was used to fit the

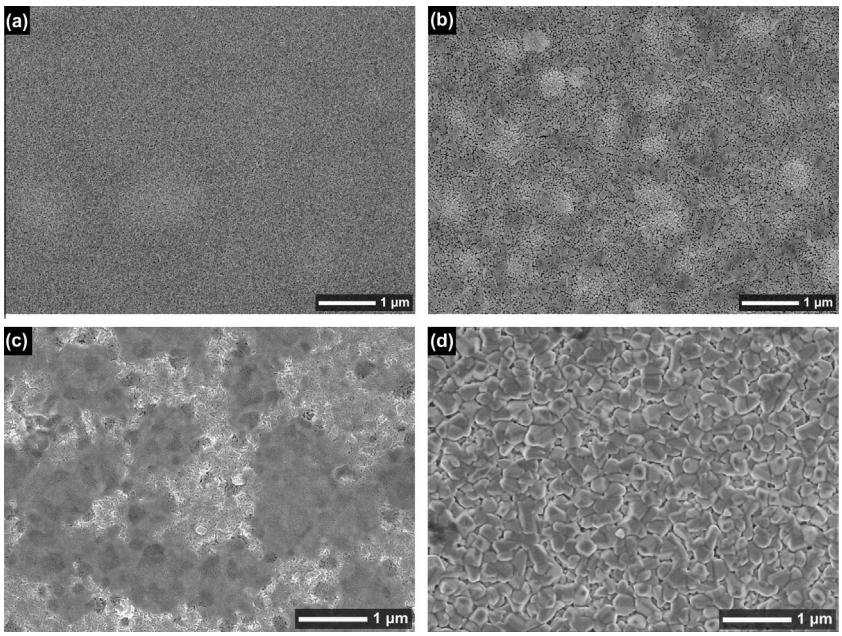

Fig. 2. FEG-SEM micrographs of CCTO thin film surfaces. (a) CF at 500 °C; (b) CF at 600 °C; (c) CF at 700 °C; (d) PF.

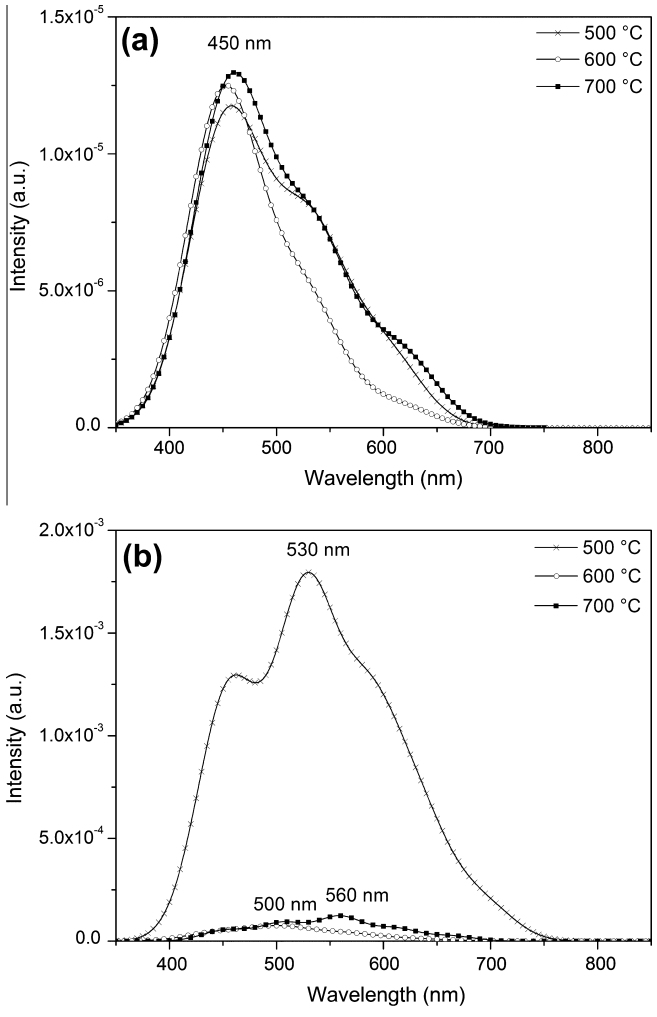

Fig. 3. PL spectra of CCTO films at different annealing conditions. (a) CF; (b) CF + PT.

Table 1
Maximum PL emission and band gap for CF and CF + PT.

Film	Maximum PL emission (nm)	E_{gap} (ev)
CF-500 °C	453	1.8
CF-500 °C + PT	526	1.1
CF-600 °C	450	1.6
CF-600 °C + PT	500	1.4
CF-700 °C	456	1.6
CF-700 °C + PT	559	1.1

PL bands which revealed the peak position and its corresponding areas (see Fig. 4). Broad band PL emission is usually observed in systems that possess different paths (involving intermediary levels) in relaxation processes [23].

In order to elucidate the effect of the air pressure on CCTO thin film, CF-700 °C and CF-700 °C + PT systems were chosen to compare the photoluminescence decomposition with PF. Both CF-700 °C and CF-700 °C + PT are in the crystalline form (see Fig. 1(f) and (g)) and were better systems to understand the pressure effects in the structure of a crystalline film. CCTO CF decomposition spectra suggest three components which form the PL emission broad band (see Fig. 4(a)). The blue component corresponds to the maximum peak emission around 456 nm which represents 56.34% of the broad PL emission. Two other components in the green and orange region were also observed with a smaller contribution to the overall PL emission. The decomposition depicted in Fig. 4(b) shows a displacement in the main emission to the green region (around 559 nm) after pressure treatment which seems to be around 59.60% of the broad emission when associated with the 505 nm peak (also the green region). Moreover, there is an increase in the orange and red regions (610 and 663 nm, respectively). A similar emission was observed in PFs (see Fig. 4(c)) which produce a green main emission at 529 nm and corresponds to about 40.34% of the PL emission. An increase in the lower energy emission (orange and red regions) was also observed in PFs which contributed 36.13% of the total PL emission.

The results of this study reveal a positive influence of pressure treatment on optical properties. Pressure leads to a decrease in CCTO thin film band gaps which stimulates PL emission at a lower energy region (a higher wavelength). Pressure provides a better

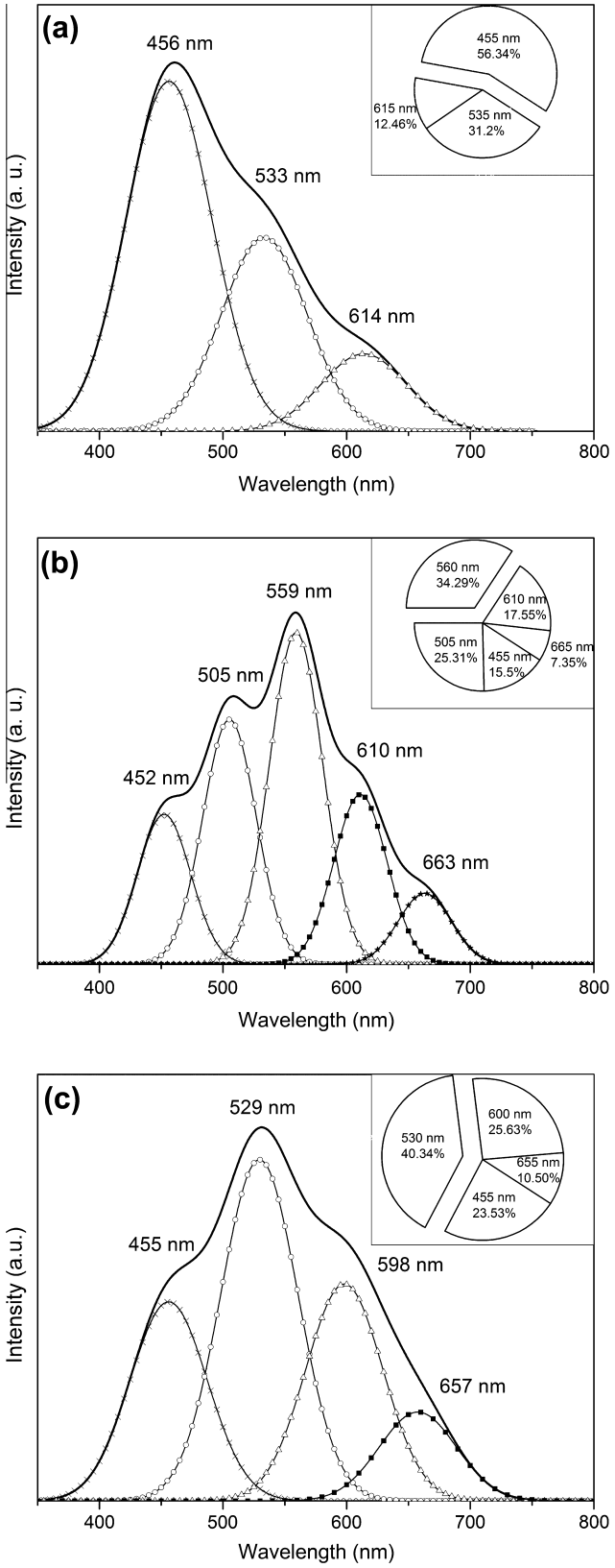

Fig. 4. Decomposition of CCTO thin film PL spectra. (a) CF-700 °C; (b) CF-700 °C + PT; (c) PF.

influence on CCTO CFs calcinated at lower temperatures due to the predominance of an amorphous phase. However, pressure is also able to affect crystalline particles; i.e., the red shift demonstrated in PFs which started from CCTO crystalline powders.

4. Conclusion

In this study, optical properties of CCTO thin films from both chemical solution and pressure depositions were evaluated. Both CFs and PFs have a porous surface, but PFs resulted in a more homogeneous and denser film surface with a larger grain size. Pressure treatment also exerted a greater influence on optical characteristics which produced a decrease in the CCTO film band gap due to the rupture of the Ti–O bonds and the genesis of intermediary energy levels inside the band gap region (overlap between valence and conduction bands). Lower band gaps and intermediate energy levels produced the PL emission red shift observed in CCTO films after pressure treatment.

Acknowledgements

The authors acknowledge the Brazilian research funding agencies of FAPESP (Grant 2009/11099-2 and CEPID 98/14324-0) and FINEP (Grant 3903/06) for their financial support.

References

[1] C.C. Homes, T. Vogt, S.M. Shapiro, S. Wakimoto, A.P. Ramirez, Science 293 (2001) 673–676.
[2] A.P. Ramirez, M.A. Subramanian, M. Gardel, G. Blumberg, D. Li, T. Vogt, S.M. Shapiro, Solid State Commun. 115 (2000) 217–220.
[3] M.A. Subramanian, D. Li, N. Duan, B.A. Reisner, A.W. Sleight, J. Solid State Chem. 151 (2000) 323–325.
[4] M.A. Subramanian, A.W. Sleight, Solid State Sci. 4 (2002) 347–351.
[5] L.S. Cavalcante, M. Anicete-Santos, J.C. Sczancoski, L.G.P. Simões, M.R.M.C. Santos, J.A. Varela, P.S. Pizani, E. Longo, J. Phys. Chem. Solids 69 (2008) 1782–1789.
[6] L.T. Canham, Appl. Phys. Lett. 57 (1990) 1046–1048.
[7] M. Anicete-Santos, L.S. Cavalcante, E. Orhan, E.C. Paris, L.G.P. Simões, M.R. Joya, I.L.V. Rosa, P.R. de Lucena, M.R.M.C. Santos, L.S. Santos-Júnior, P.S. Pizani, E.R. Leite, J.A. Varela, E. Longo, Chem. Phys. 316 (2005) 260–266.
[8] T. Kyômen, R. Sakamoto, N. Sakamoto, S. Kunugi, M. Itoh, Chem. Mater. 17 (2005) 3200–3204.
[9] E.R. Leite, F.M. Pontes, E.C. Paris, C.A. Paskocimas, E.J.H. Lee, E. Longo, P.S. Pizani, J.A. Varela, V. Mastelaro, Adv. Mater. Opt. Electron. 10 (2000) 235–240.
[10] A.T. de Figueiredo, S. de Lazaro, E. Longo, E.C. Paris, J.A. Varela, M.R. Joya, P.S. Pizani, Chem. Mater. 18 (2006) 2904–2911.
[11] T.C. Hufnagel, Nat. Mater. 3 (2004) 666–667.
[12] P.S. Salmon, Nat. Mater. 1 (2002) 87–88.
[13] I.V. Rosa, L. Oliveira, E. Longo, J. Varela, J. Fluoresc. 21 (2011) 975–981.
[14] M.H. Whangbo, M.A. Subramanian, Chem. Mater. 18 (2006) 3257–3260.
[15] M.A. Ramirez, A.Z. Simões, A.A. Felix, R. Tararam, E. Longo, J.A. Varela, J. Alloys Comp. 509 (2011) 9930–9933.
[16] S. Cava, T. Sequinel, S.M. Tebcherani, S.R. Lazaro, S.A. Pianaro, J.A. Varela, Thin Solid Films 518 (2010) 5889–5891.
[17] S. Cava, T. Sequinel, S.M. Tebcherani, M.D. Michel, S.R. Lazaro, S.A. Pianaro, J. Alloys Comp. 484 (2009) 877–881.
[18] S. Cava, T. Sequinel, S.M. Tebcherani, M.D. Michel, C.M. Lepienski, J.A. Varela, J. Non-Cryst. Solids 356 (2010) 215–219.
[19] T. Sequinel, S. Cava, J.O. Pimenta, S.A. Pianaro, S.M. Tebcherani, J.A. Varela, Ceram. Int. 37 (2011) 1533–1536.
[20] P. Kubelka, F. Munk-Aussig, Für. Technol. Phys. 12 (1931) 593–601.
[21] F.A. Kröger, H.J. Vink, J. Phys. Chem. Solids 5 (1958) 208–223.
[22] F. Moura, A.Z. Simões, R.C. Deus, M.R. Silva, J.A. Varela, E. Longo, Ceram. Int. 39 (2013) 3499–3506.
[23] L.H. Oliveira, A.P. de Moura, T.M. Mazzo, M.A. Ramírez, L.S. Cavalcante, S.G. Antonio, W. Avansi, V.R. Mastelaro, E. Longo, J.A. Varela, Mater. Chem. Phys. 136 (2012) 130–139.